Biophysical Journal, Volume *111*

Supplemental Information

MreB Orientation Correlates with Cell Diameter in *Escherichia coli*

Nikolay Ouzounov, Jeffrey P. Nguyen, Benjamin P. Bratton, David Jacobowitz, Zemer Gitai, and Joshua W. Shaevitz

Supplemental Information

MreB orientation determines cell diameter in *Escherichia coli*

Nikolay Ouzounov[1], Jeffrey Nguyen[2], Benjamin Bratton[1,3], David Jacobowitz[2], Zemer Gitai[1], Joshua W. Shaevitz[2,3*]

[1]Department of Molecular Biology, Princeton University, Princeton, NJ 08544, USA

[2]Department of Physics, Princeton University, Princeton, NJ 08544, USA

[3]Lewis-Sigler Institute for Integrative Genomics

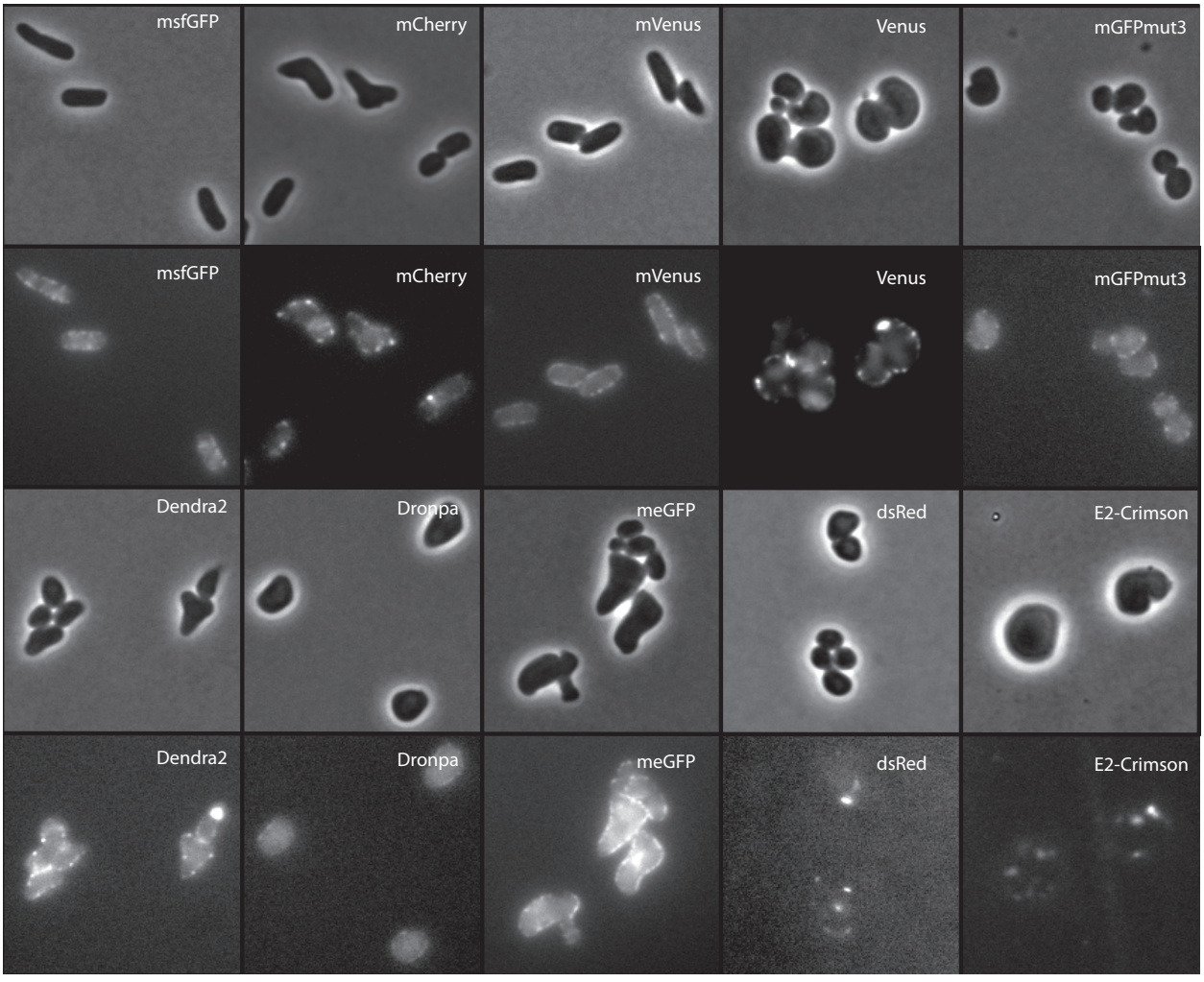

Figure S1. MG1655 *mreB* deletion strain was complemented with a plasmid containing the MreB operon in which MreB is labeled with different fluorescent proteins. The florescent proteins that have been previously shown to cause the least amount of dimerization are msfGFP, mVenus, mGFPmut3, Dendra 2, Dronpa, and meGFP. msfGFP was best able to complement rod shape and had optimal quantum yield for prolonged imaging. Venus is known to form dimers

and both dsRed and E2-Crimson form tetramers. Amino acid sequences are listed in the supplementary table below. Imaging was performed using a Nikon (Melville, NY) TI-E microscope using a 100X Nikon Plan Apo objective (NA = 1.4), Prior Lumen 200 Pro illumination, and 89014VS dichroic mirror. Images were acquired with an Andor Clara camera using NIS-Elements software.

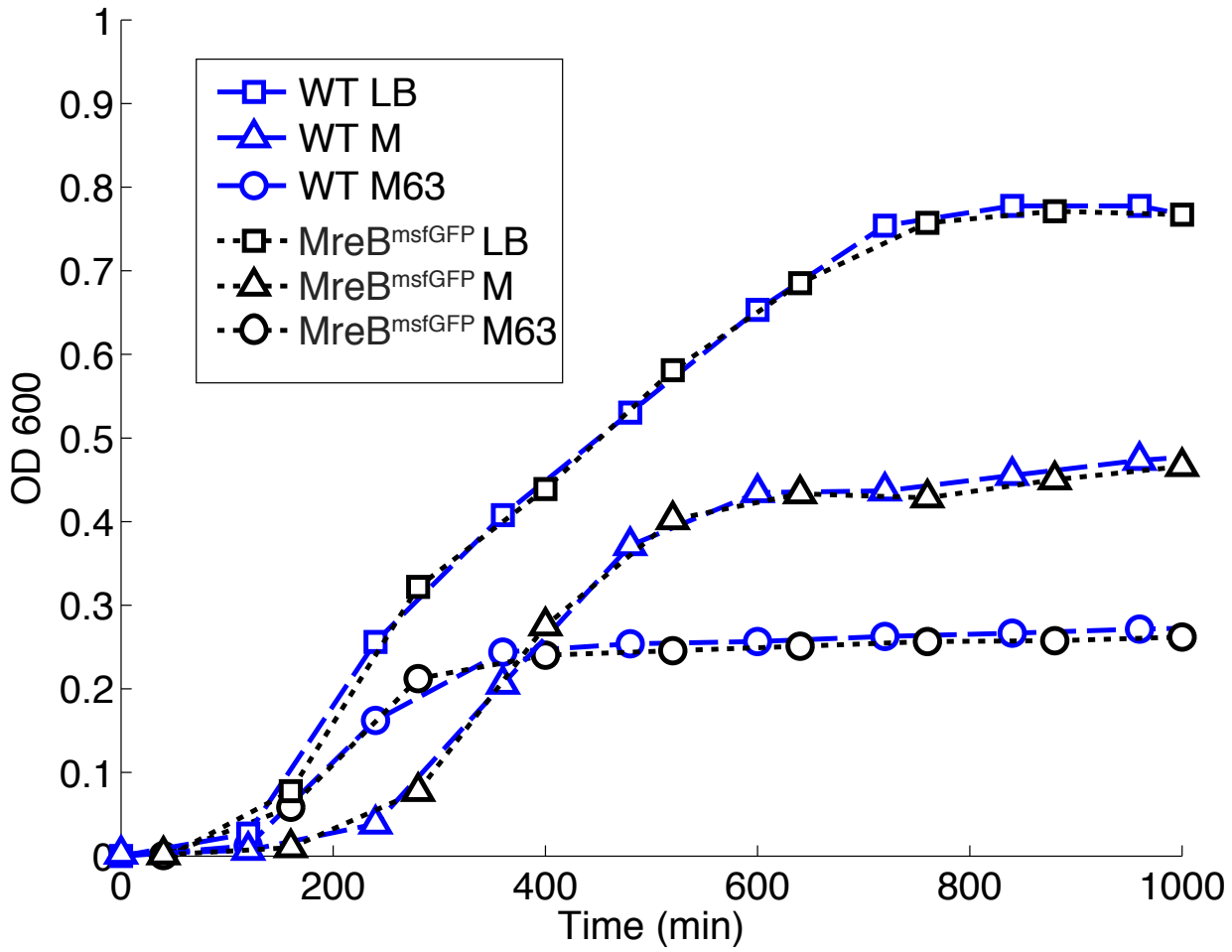

Figure S2. Comparison of OD growth curves between *E. coli* expressing native MreB and *E. coli* expressing tagged MreB^{msfGFP} integrated in the native *mreB* locus. Cells were grown in LB, M63 media with glucose and casamino acids, and in M media. There is close agreement between the two strains in all types of media. Data was averaged over 3 replicates.

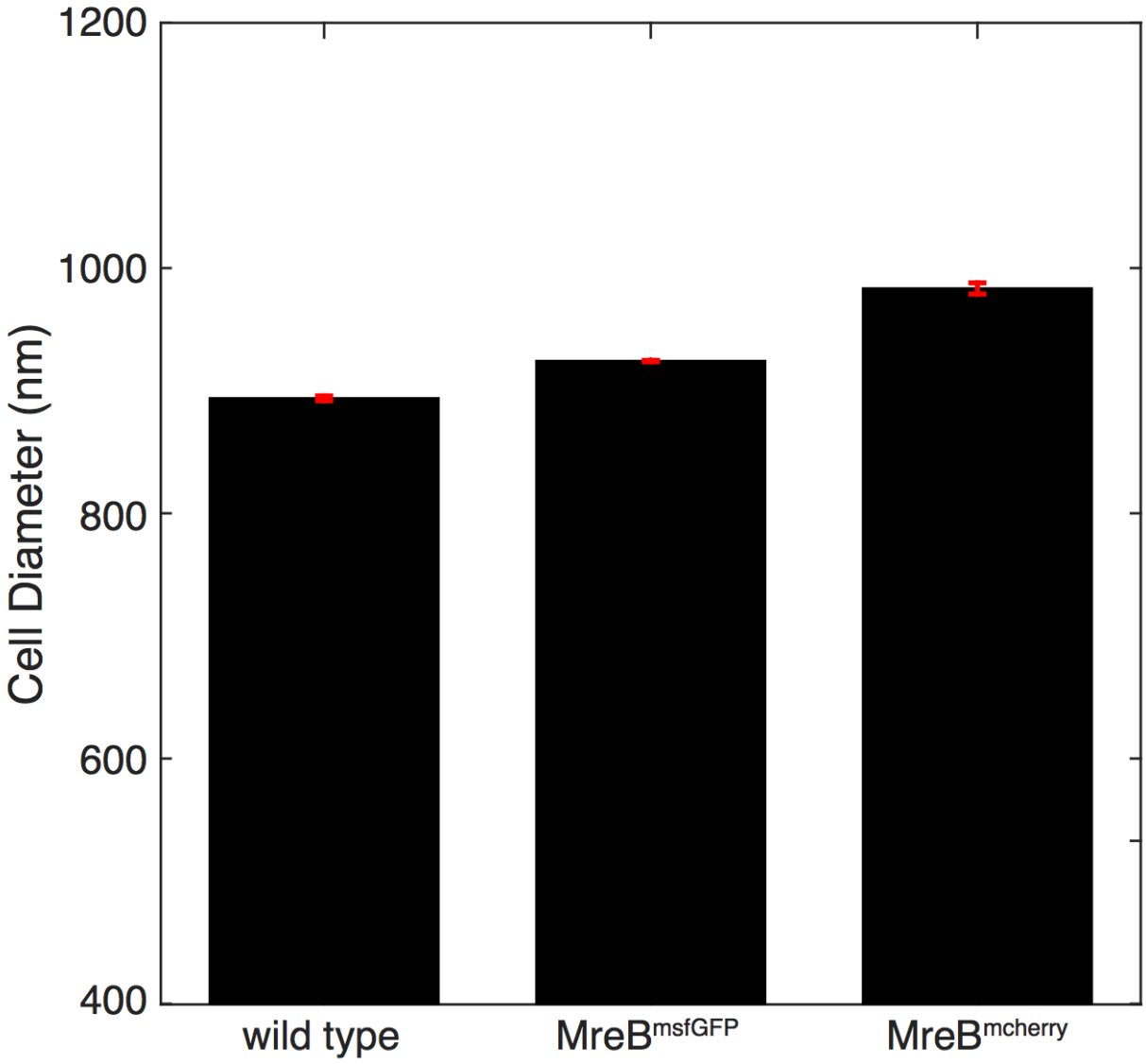

Figure S3. Average cell diameters for *E. coli* expressing native MreB (n=645), MreB^{msfGFP} (n= 459), and MreB^{mcherry} (n=372). The average diameters were 893±3 nm for the unlabeled strain, 934±6 nm for MreB^{msfGFP} , and 983 ±5 nm for MreB^{mcherry}. Cells were grown in M63 media with casamino acids.

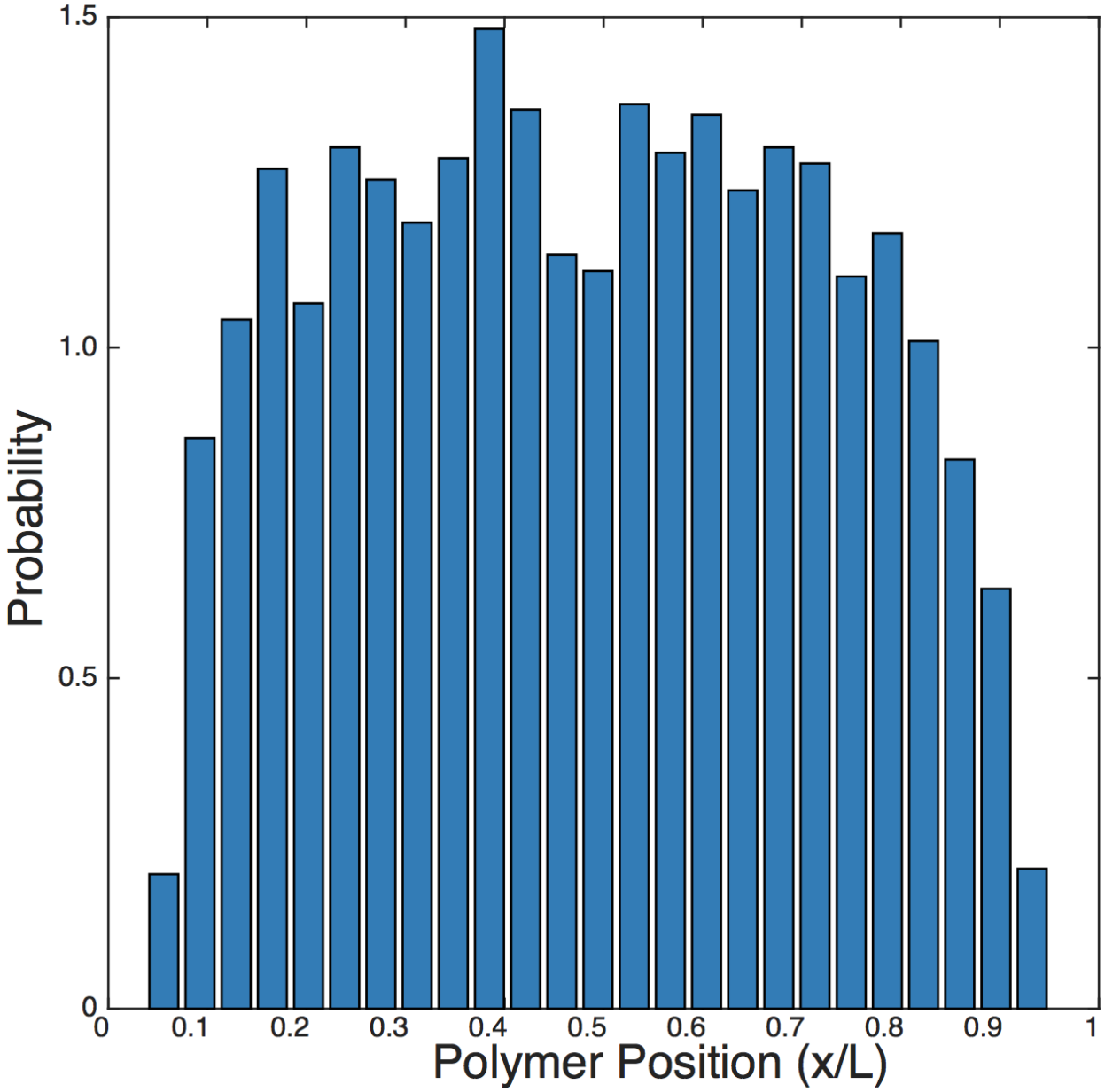

Figure S4. A distribution of MreB polymer positions as a function of percentage length along the cell in *E. coli* expressing $MreB^{msfGFP}$. The polymers are excluded near the poles of the cells. Data is collected from 459 cells, each with an average of 7.3 polymers detected.

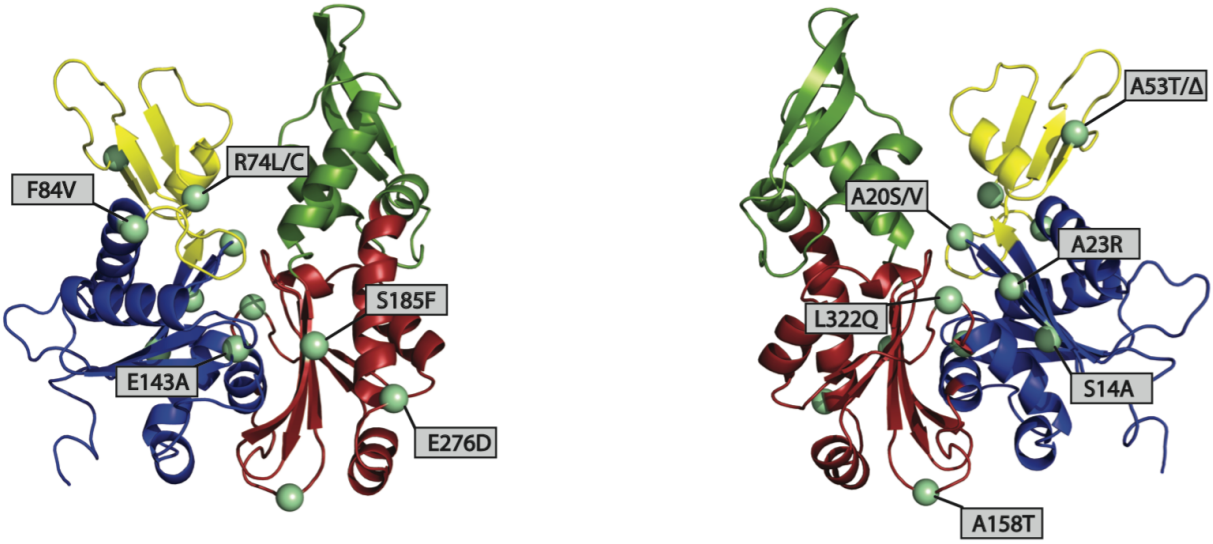

Figure S5. Amino acid substitutions are found spanning subdomains IA (Blue), IB (Yellow), and IIA (Red) (1). Some residues are hit more than once. *E. coli* MreB structure was generated using the Phyre2 server (2).

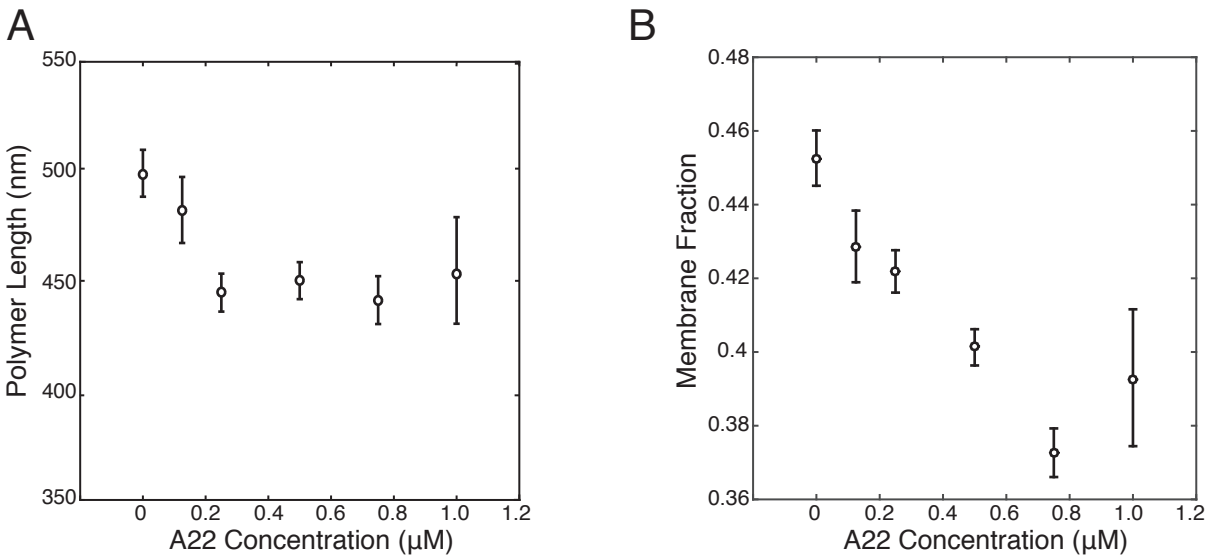

Figure S6. (A) MreB polymer length as a function of A22 concentration for cells expressing MreB^{msfGFP}. Cells were grown in the presence different sub-lethal concentrations of the MreB polymerization inhibitor A22 for multiple generations and imaged in exponential growth phase. (B) Membrane fraction plotted against A22 concentration for E. coli expressing MreB^{msfGFP}. At increasing A22 concentrations, the fraction of fluorescent signal that is localized near the membrane decreases. Error bars indicate 80% confidence intervals for both panels.

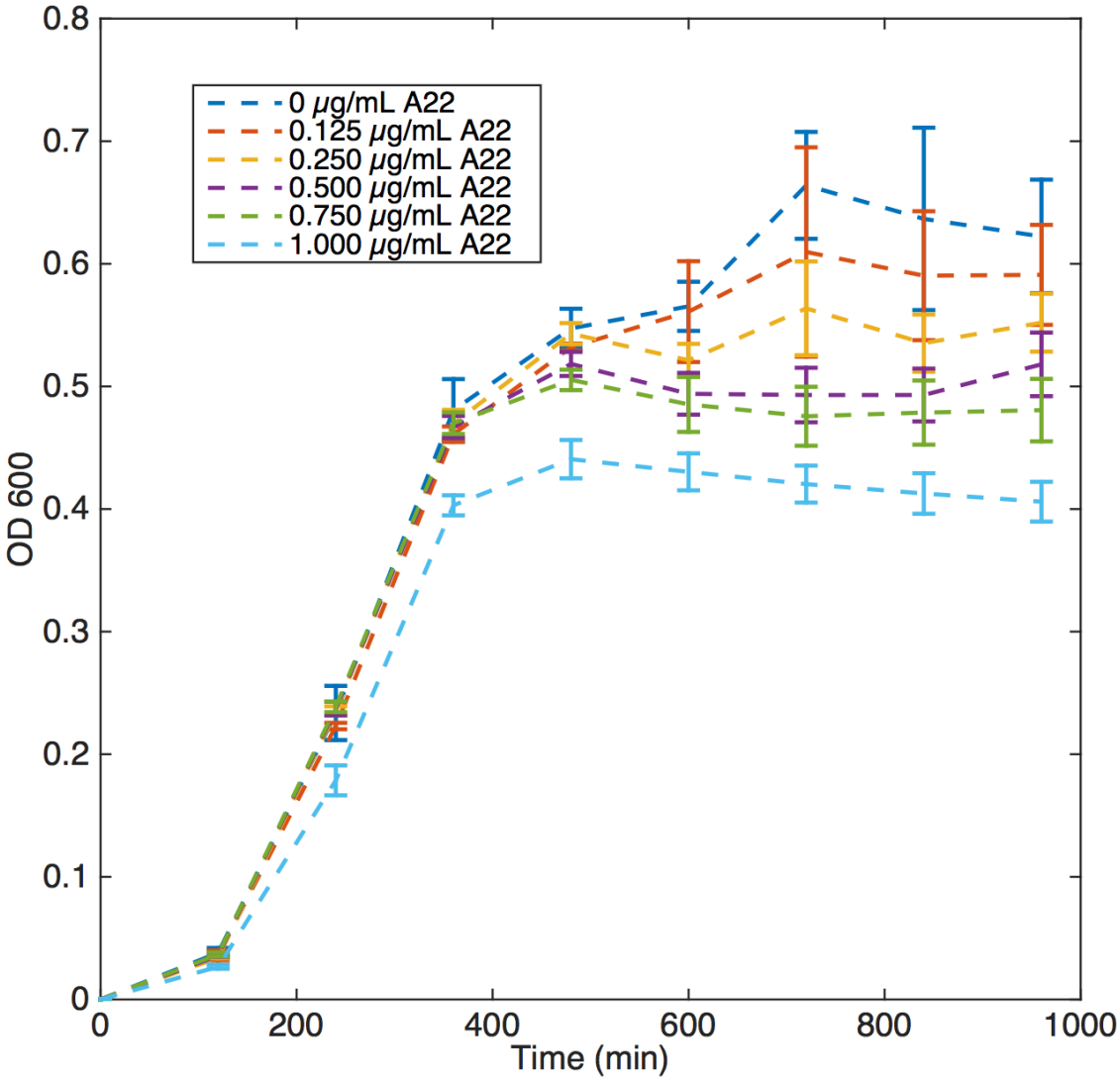

Figure S7. OD600 growth curves for *E. coli* grown at different sub-lethal concentrations of the MreB polymerization inhibitor A22. Cells grown at higher concentrations of A22 have lower log phase growth rates and lower steady state OD.

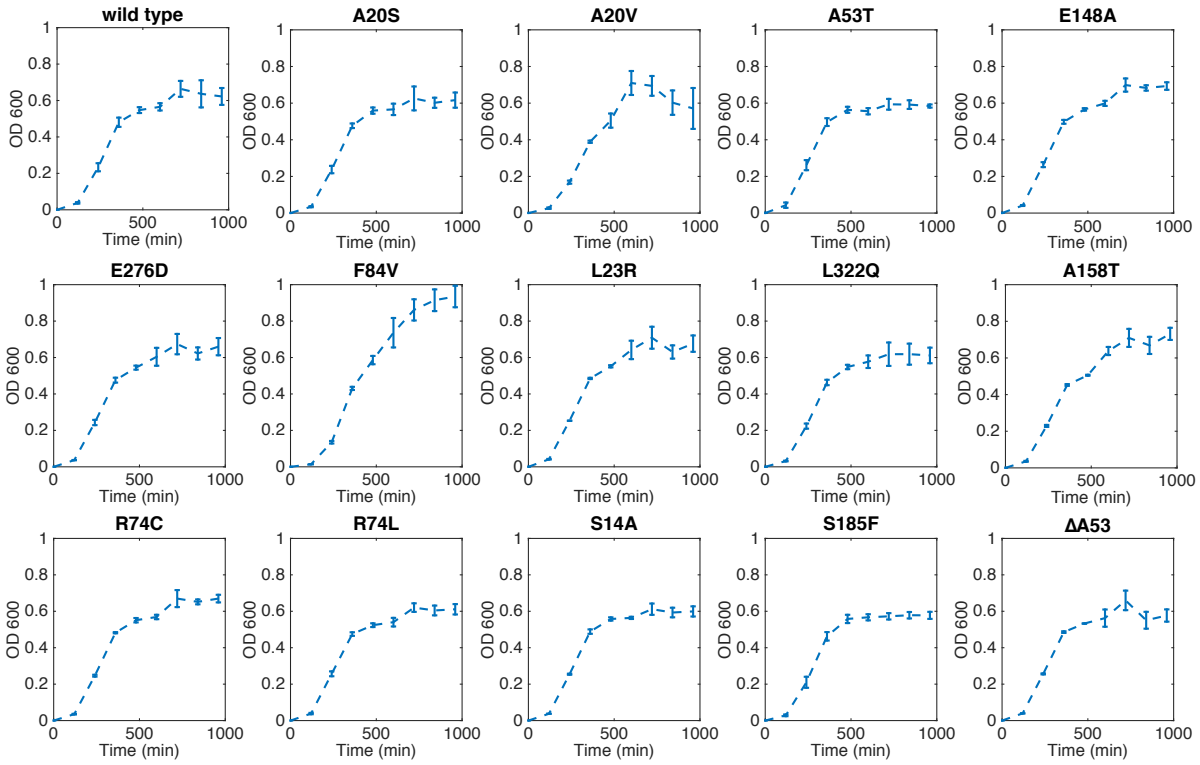

Figure S8. OD600 growth curves for the *E. coli* MreB mutants used in this study. All mutants except F84V have comparable growth rates and steady state ODs. F84V the slowest growth rate yet reaches the highest final OD.

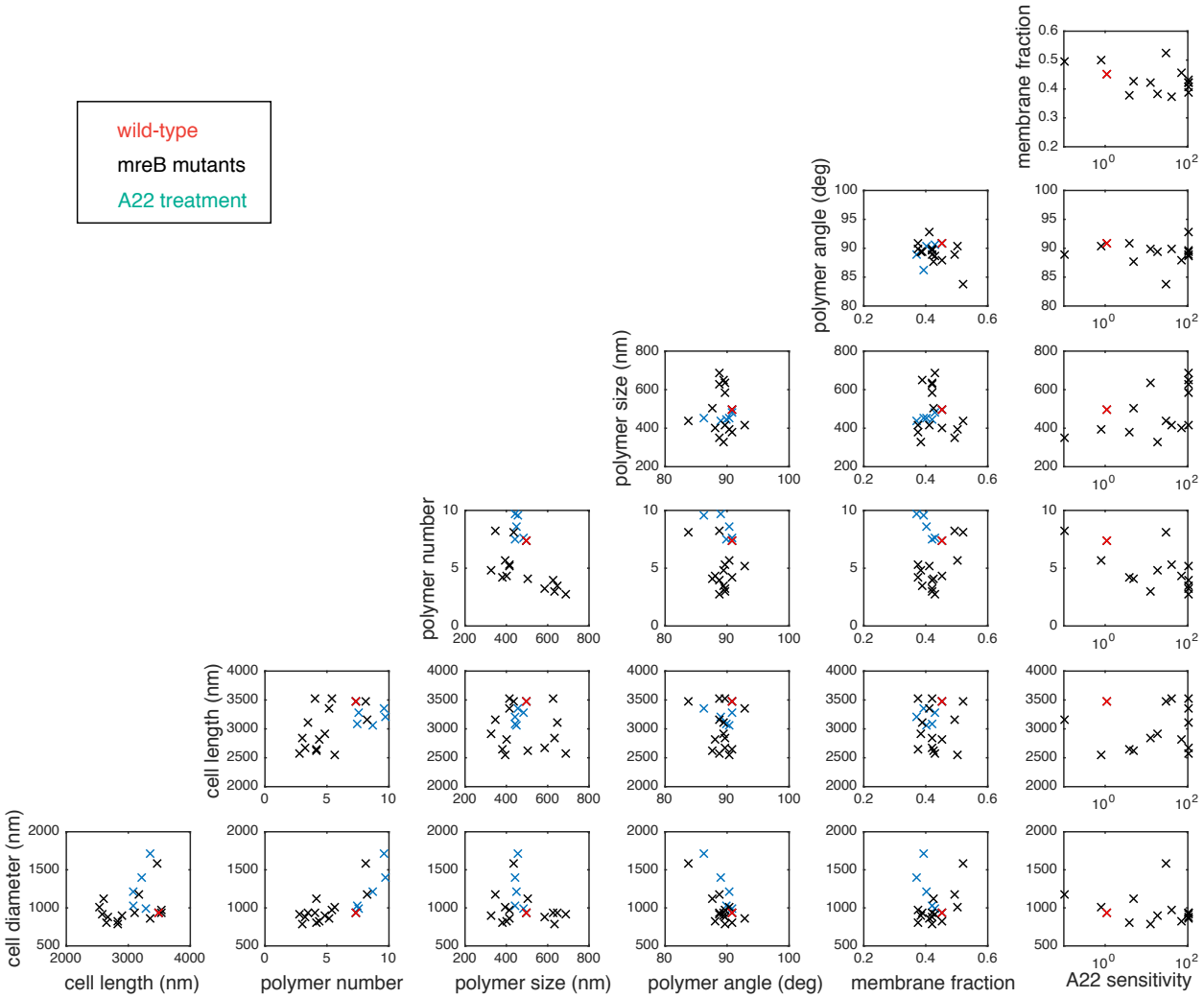

Figure S9. Scatter plots of all data used to generate correlation maps in Figure 5. Green points indicate the A22 treatment conditions, black points are from MreB point mutants, and the red point is from untreated MreB^{msfGFP}. As with Figure 4B, A22 sensitivity measurements are expressed as a fold change from wild-type and are capped at 100×.

MreB	MLKKFRGMFSNDLSIDLGTANTLIYVKGQGIVLNEPSVVAIRQDRAGSPKSVAAVGHDAK QMLGRTPGNIAAIRPMKDGVIADFFVTEKMLQHFIKQVHSNSFMRPSPRVLVCVPVGAT QVERRAIRESAQGAGAREVFLIEEPMAAAIGAGLPVSEATGSMVVDIGGGTTEVAVISLN GVVYSSSVRIGGDRFDEAIINYVRRNYGSLIGEATAERIKHEIGSAYPGSGSSxxxxxSGAP GDEVREIEVRGRNLAEGVPRGFTLNSNEILEALQEPLTGIVSAVMVALEQCPPELASDISE RGMVLTGGGALLRNLDRLLMEETGIPVVVAEDPLTCVARGGGKALEMIDMHGGDLFSEE
mCherry	MVSKGEEDNMAIIKEFMRFKVHMEGSVNGHEFEIEGEGEGRPYEGTQTAKLKVTKGGPL PFAWDILSPQFMYGSKAYVKHPADIPDYLKLSFPEGFKWERVMNFEDGGVVTVTQDSSL QDGEFIYKVKLRGTNFPSDGPVMQKKTMGWEASSERMYPEDGALKGEIKQRLKLKDGG HYDAEVKTTYKAKKPVQLPGAYNVNIKLDITSHNEDYTIVEQYERAEGRHSTGGMDELYK
msfGFP	SKGEELFTGVVPILVELDGDVNGHKFSVRGEGEGDATNGKLTLKFICTTGKLPVPWPTLV TTLTYGVQCFSRYPDHMKQHDFFKSAMPEGYVQERTISFKDDGTYKTRAEVKFEGDTLV NRIELKGIDFKEDGNILGHKLEYNFNSHNVYITADKQKNGIKANFKIRHNVEDGSVQLADH YQQNTPIGDGPVLLPDNHYLSTQSKLSKDPNEKRDHMVLLEFVTAAGITHGMDELYK
mVenus	MVSKGEELFTGVVPILVELDGDVNGHKFSVSGEGEGDATYGKLTLKLICTTGKLPVPWPT LVTTLGYGLQCFARYPDHMKQHDFFKSAMPEGYVQERTIFFKDDGNYKTRAEVKFEGD TLVNRIELKGIDFKEDGNILGHKLEYNYNSHNVYITADKQKNGIKANFKIRHNIEDGGVQLA DHYQQNTPIGDGPVLLPDNHYLSYQSKLSKDPNEKRDHMVLLEFVTAAGITLGMDELYK
Venus	MVSKGEELFTGVVPILVELDGDVNGHKFSVSGEGEGDATYGKLTLKLICTTGKLPVPWPT LVTTLGYGLQCFARYPDHMKQHDFFKSAMPEGYVQERTIFFKDDGNYKTRAEVKFEGD TLVNRIELKGIDFKEDGNILGHKLEYNYNSHNVYITADKQKNGIKANFKIRHNIEDGGVQLA DHYQQNTPIGDGPVLLPDNHYLSYQSALSKDPNEKRDHMVLLEFVTAAGITLGMDELYK
mGFPmut3	SKGEELFTGVVPILVELDGDVNGHKFSVSGEGEGDATYGKLTLKFICTTGKLPVPWPTLV TTFGYGVQCFARYPDHMKQHDFFKSAMPEGYVQERTIFFKDDGNYKTRAEVKFEGDTL VNRIELKGIDFKEDGNILGHKLEYNYNSHNVYIMADKQKNGIKVNFKIRHNIEDGSVQLAD HYQQNTPIGDGPVLLPDNHYLSTQSKLSKDPNEKRDHMVLLEFVTAAGITHGMDELYK
meGFP	SGGGGSKVSKGEELFTGVVPILVELDGDVNGHKFSVSGEGEGDATYGKLTLKFICTTGK LPVPWPTLVTTLTYGVQCFSRYPDHMKQHDFFKSAMPEGYVQERTIFFKDDGNYKTRA EVKFEGDTLVNRIELKGIDFKEDGNILGHKLEYNYNSHNVYIMADKQKNGIKVNFKIRHNIE DGSVQLADHYQQNTPIGDGPVLLPDNHYLSTQSKLSKDPNEKRDHMVLLEFVTAAGITL GMDELYK
Dronpa	VIKPDMKIKLRMEGAVNGHPFAIEGVGLGKPFEGKQSMDLKVKEGGPLPFAYDILTTVFC YGNRVFAKYPENIVDYFKQSFPEGYSWERSMNYEDGGICNATNDITLDGDCYIYEIRFDG VNFPANGPVMQKRTVKWEPSTEKLYVRDGVLKGDVNMALSLEGGGHYRCDFKTTYKA KKVVQLPDYHFVDHHIEIKSHDKDYSNVNLHEHAEAHSELPRQAK
Dendra2	MNTPGINLIKEDMRVKVHMEGNVNGHAFVIEGEGKGKPYEGTQTANLTVKEGAPLPFSY DILTTAVHYGNRVFTKYPEDIPDYFKQSFPEGYSWERTMTFEDKGICTIRSDISLEGDCFF QNVRFKGTNFPPNGPVMQKKTLKWEPSTEKLHVRDGLLVGNINMALLLEGGGHYLCDF KTTYKAKKVVQLPDAHFVDHRIEILGNDSDYNKVKLYEHAVARYSPLPSQVW
E2-Crimson	DSTENVIKPFMRFKVHMEGSVNGHEFEIEGVGEGKPYEGTQTAKLQVTKGGPLPFAWDI LSPQFFYGSKAYIKHPADIPDYLKQSFPEGFKWERVMNFEDGGVVTVTQDSSLQDGTLIY HVKFIGVNFPSDGPVMQKKTLGWEPSTERNYPRDGVLKGENHMALKLKGGGHYLCEFK SIYMAKKPVKLPGYHYVDYKLDITSHNEDYTVVEQYERAEARHHLFQ
dsRed	RSSKNVIKEFMRFKVRMEGTVNGHEFEIEGEGEGRPYEGHNTVKLKVTKGGPLPFAWDI LSPQFQYGSKVYVKHPADIPDYKKLSFPEGFKWERVMNFEDGGVVTVTQDSSLQDGCFI YKVKFIGVNFPSDGPVMQKKTMGWEASTERLYPRDGVLKGEIHKALKLKDGGHYLVEFK SIYMAKKPVQLPGYYYVDSKLDITSHNEDYTIVEQYERTEGRHHLFL

Table S1. The amino acid sequences of MreB and the different fluorescent proteins used in this study. Linker amino acid sequences are highlighted in yellow and the location of the fluorescent protein is in red.

Supplemental References

1. van den Ent F, Amos LA, & Lowe J (2001) Prokaryotic origin of the actin cytoskeleton. *Nature* 413(6851):39-44.
2. Kelley LA & Sternberg MJ (2009) Protein structure prediction on the Web: a case study using the Phyre server. *Nature protocols* 4(3):363-371.